# PCHE-type steam generator sizing analysis for nuclear-powered ships

### Taeseok Kim a\*

Department of Nuclear Engineering, Jeju National University, Jeju, 63243, Republic of Korea \*Corresponding author: tkim@jejunu.ac.kr

\*Keywords: Marine Propulsion, Steam Generator, PCHE

#### 1. Introduction

The design of marine nuclear reactors are critically constrained by the inherent limitations of onboard space. Unlike their land-based, maritime applications demand compact and lightweight systems to ensure operational efficiency and safety within a confined vessel footprint.

Significant progress has been made in the development of Small Modular Reactors (SMRs), which offer enhanced safety, economic benefits, and reduced physical size compared to traditional large-scale nuclear power plants. These advancements have contributed to the miniaturization of various reactor components. However, the steam generator often remains a considerable volumetric challenge.

Recently, there has been a growing interest in exploring Printed Circuit Heat Exchangers (PCHEs) as a viable alternative for steam. PCHEs are known for their compactness, high heat transfer efficiency, and robust design, making them an attractive candidate to overcome the volumetric limitations posed by conventional steam generators.

Building upon this emerging research, the present study aims to contribute to the advancement of marine nuclear reactor design. Specifically, this paper focuses on performing a preliminary sizing analysis for a PCHE-type steam generator tailored for nuclear-powered ships, considering the stringent space and performance requirements unique to this environment.

### 2. Analysis methods

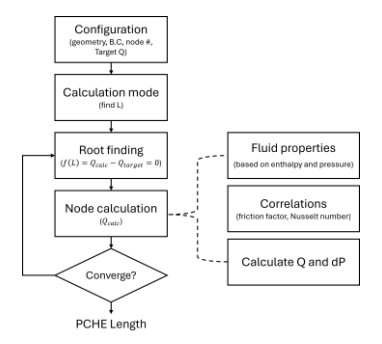


Fig. 1. Calculation flow chart for PCHE sizing

The sizing analysis for the PCHE-type steam generator is based on the heat balance equation. Given the compact nature of PCHEs, which feature mini channels typically around 2 mm in diameter, a detailed

understanding of fluid flow and heat transfer within these geometries is crucial. This study models the PCHE with counter-current flow. The core of the calculation involves equating the enthalpy change of the hot fluid to the enthalpy change of the cold fluid, both of which are equal to the total heat transfer rate across the mini channels. This heat transfer rate is determined through a combination of selected empirical correlations. The entire calculation process follows a sequential flow, which is elaborated in Fig. 1.

#### 2.1 Correlations

Accurate prediction of heat transfer and pressure drop necessitates the careful selection of appropriate correlations. For single-phase regions, established correlations such as the Dittus-Boelter equation for heat transfer and the Churchill friction factor for pressure drop are employed. However, the two-phase flow regime requires more specialized and validated approaches. This study systematically selected four crucial two-phase correlations following extensive evaluation against available experimental data.

For the Boiling Heat Transfer Coefficient (BHTC), a comprehensive review of correlations was performed [1-7]. These were compared with experimental data specifically for mini-channel boiling [8].

Regarding Critical Heat Flux (CHF), two primary tabular correlations from 1986 and 2006 were considered [9,10]. To apply to mini channels, these correlations were evaluated in conjunction with two correction factors: Duckler correction and Wong correction factor [11,12].

Predicting heat transfer in the Post-Dryout (PDO) regime presents significant challenges due to the complex flow patterns involved. The previous correlations considered included [13-15].

Finally, for Two-Phase Pressure Drop, various correlations were evaluated [16-22] and compared with experimental data [12].

### 2.2 Conditions

The sizing analysis was performed under specific geometrical and thermal-hydraulic conditions, which were carefully chosen to reflect realistic marine nuclear reactor design parameters and PCHE characteristics. The reference PCHE block dimensions were set to 0.6 meters in height and 0.6 meters in width, consistent with typical Heatric PCHE designs. The primary objective of this

sizing analysis is to determine the optimal length of the PCHE block. Based on detailed geometrical calculations, each PCHE block is designed to accommodate 250 channels along the width axis and 400 channels along the height axis, resulting in a total of 100,000 mini-channels within a single PCHE block. These channels are arranged in a 1:1 hot/cold configuration, meaning there are 50,000 hot channels and 50,000 cold channels.

The operating conditions were derived from a representative marine nuclear reactor design. The total thermal power output required from the steam generator is 200 MW. The hot fluid (primary coolant) flow rate is 997.5 kg/s, while the cold fluid (secondary coolant, water) flow rate is 111.52 kg/s. The cold side inlet subcooling is maintained at 20 K, and the hot side inlet temperature is specified as 598.15 K. To evaluate the flexibility and scalability of the PCHE-type steam generator, the sizing analysis was performed for varying numbers of PCHE blocks, specifically considering configurations with 2, 3, 4, 5, 6, and 8 PCHE blocks to assess the impact on overall length and performance.

#### 3. Results

### 3.1 Correlation selection

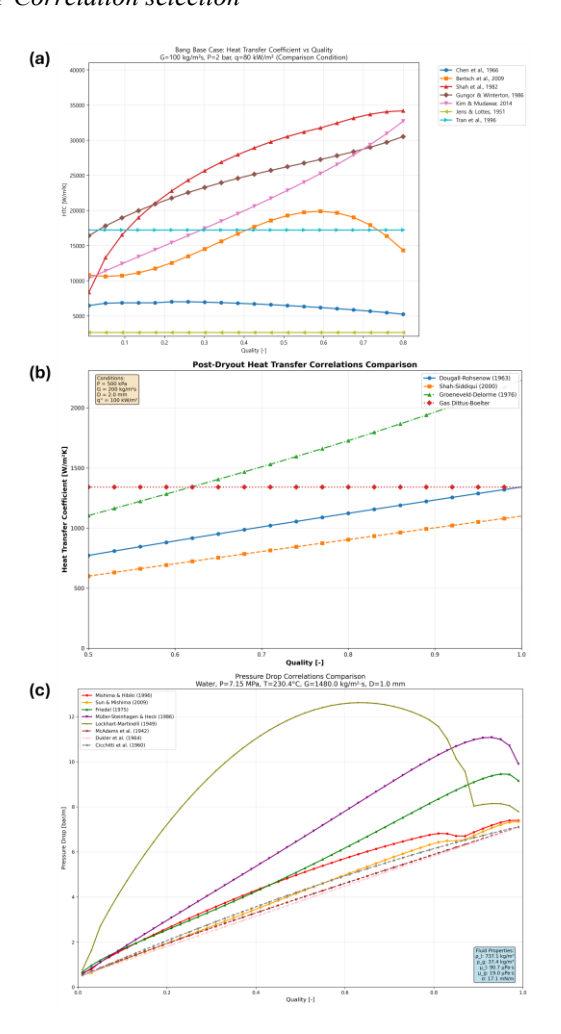


Fig. 2. Correlation values by quality (a) BHTC (b) Post dryout HTC (c) Two-phase pressure drop

BHTC correlations revealed divergent trends among the candidates when compared to experimental data (Fig.2 (a)). Specifically, the data [8] indicated BHTC values ranging from approximately 10,000 W/m²K to 30,000 W/m²K across varying qualities. Among the correlations assessed, the Kim & Mudawar correlation demonstrated the most accurate and consistent fit with this experimental data.

In PDO correlations, the analysis indicated that while the overall trends predicted by the various correlations were largely similar, there were observable differences in the precise range of predicted HTCs (Fig.2 (b)). Considering their historical use and robustness, the Groeneveld-Delorme correlation was selected for its proven reliability, particularly in the absence of specific mini-channel experimental data for this regime.

For Two-Phase Pressure Drop correlations, the examined models generally exhibited comparable trends, although their predicted pressure ranges showed notable differences (Fig.2 (c)). Both the Cicchitti HEM correlation and the Sun & Mishima correlation provided strong fits to the experimental data. the Sun & Mishima correlation was ultimately chosen as the most appropriate and accurate model for predicting two-phase pressure drop in this PCHE sizing analysis.

# 3.2 Sensitivity of the number of PCHE

The number of PCHE blocks significantly influences the overall thermal-hydraulic behavior, leading to distinct profiles across various operating parameters. To illustrate these differences, a comparative analysis was conducted for key variables along the normalized length of the PCHE. Specifically, the temperature profile is presented in Fig. 3(a), the pressure drop profile in Fig. 3(b), and the heat flux and total heat transfer rate in the cold side in Fig. 3(c).

Observing the temperature profiles (Fig. 3(a)), the hot side fluid, moving in a counter-current direction, experiences a decrease in temperature as it transfers heat from a normalized length of 1.0 towards 0.0. Since the hot side fluid remains in a single-phase state throughout its passage, its temperature change is affected mainly by the HTC of the cold side. Interestingly, for cases with a higher number of PCHE blocks, specifically n=6 and n=8, the region where heat transfer performance significantly increases, where the cold side exhibits excellent heat transfer—appears later and occupies a smaller portion of the PCHE length. This behavior is primarily attributed to the dynamics of the cold side, which will be further discussed in subsequent sections. The cold side temperature graph clearly illustrates the progression from a subcooled liquid state, through a saturation plateau, and finally into a superheated steam phase.

The pressure drop profiles (Fig. 3(b)) indicate that the hot side generally experiences a higher pressure drop compared to the cold side, primarily due to its higher Reynolds number. On the cold side, the pressure drop increases considerably within the two-phase flow regime, and a distinct transition region is evident as the fluid

converts from a two-phase mixture to single-phase superheated vapor. Overall, configurations with a fewer number of PCHE blocks, which correspond to higher mass fluxes per channel, show a more pronounced impact on the total pressure drop.

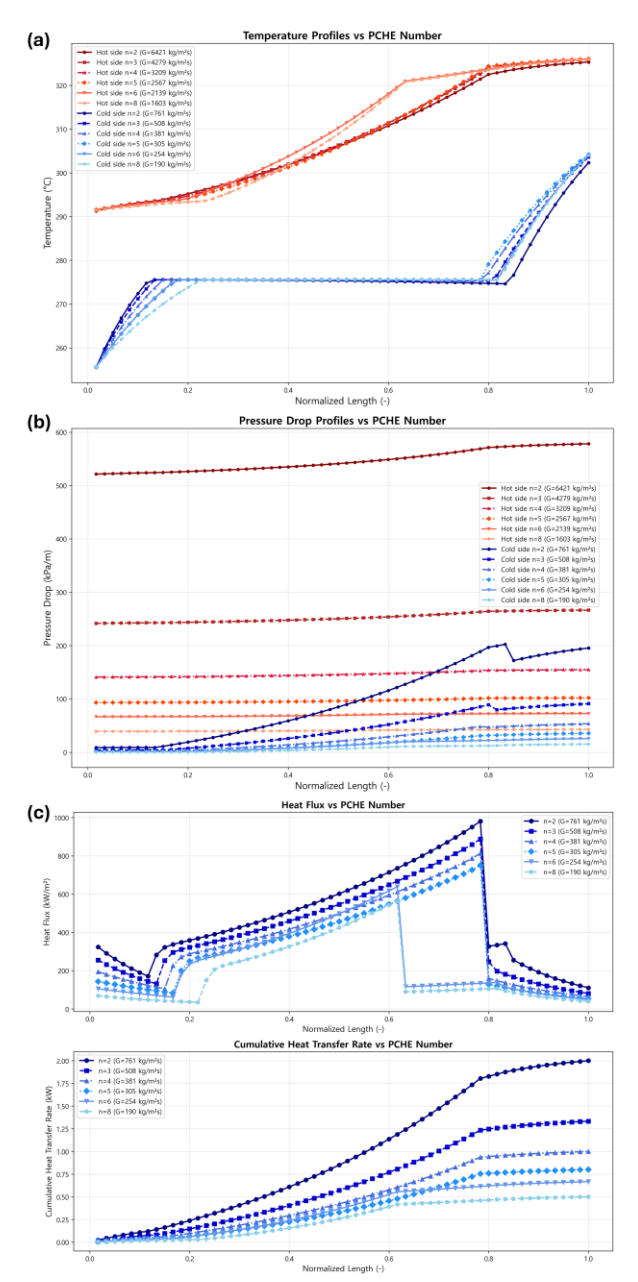


Fig. 3. The effects of the number of PCHE with normalized length (a) temperature profiles (b) pressure drop profiles (c) heat flux and total heat transfer rate in cold side

Analyzing the cold side heat flux profiles (Fig. 3(c)) provides clear insights into the different regimes. In all cases, the transition from a subcooled liquid to the saturated boiling state is distinctly visible. Following this, a peak heat flux is observed, after which there is a sharp decrease, indicating a transition to the post-dryout regime. However, in the n=6 and n=8 cases, this decrease in heat flux occurs noticeably earlier than in other cases. This phenomenon is directly linked to the CHF. The CHF model incorporated in this study utilizes a diameter

correction factor proposed by Tanase et al. [23]. This correction factor exhibits a sharp change in its coefficient at a mass flux of 250 kg/m²s. As the number of PCHE blocks changes, the mass flux per channel is altered, leading to the application of this correction factor and, consequently, a significant shift in the CHF location, which is clearly depicted in the graph.

# 3.3 Overall trends with the number of PCHE

Fig. 4 summarizes the key performance indicators—pressure drop, average HTC, power density, and PCHE volume and length—as a function of the number of PCHE blocks.

From the pressure drop graph in Fig. 4(a), it is evident that the hot side consistently exhibits a higher pressure drop compared to the cold side. A clear trend of decreasing pressure drop is observed as the number of PCHE blocks increases. This reduction is primarily attributed to the lower fluid velocity per channel and the decrease in the overall length of the PCHE required for heat exchange.

The average HTC for both hot and cold sides, shown in Fig. 4(b), generally decreases as the number of PCHE blocks increases. This is because a larger number of blocks leads to a lower mass flux per channel, which in turn reduces the overall heat transfer coefficient. A notable sharp decrease in the cold side HTC is observed as the number of PCHE blocks transitions from 5 to 6. This significant drop is a direct consequence of the change in the CHF correlation's behavior, specifically relating to the diameter correction factor and its sensitivity to mass flux, as discussed previously.

The power density graph in Fig. 4(c) illustrates a clear inverse relationship with the number of PCHE blocks; power density decreases as the number of blocks increases. This suggests that configurations with fewer PCHE blocks achieve a higher power density because the higher mass flow rates per channel result in a higher average HTC, leading to more efficient heat removal per unit volume. This observation is intrinsically linked to the PCHE length presented in Fig. 4(d). While a reduction in the number of PCHE blocks necessitates an increase in the overall length to achieve the required heat removal, the enhanced HTC due to higher fluid velocities in fewer channels appears to be the dominant factor in achieving higher power density.

In summary, a smaller number of PCHE blocks generally facilitates more efficient heat removal as characterized by higher power density and HTC. However, this comes at the cost of increased pressure drop. It is crucial to note that beyond these thermal-hydraulic considerations, comprehensive design optimization would also need to incorporate additional engineering perspectives, such as limitations on piping velocities, requirements for equipment cleaning and maintenance, and overall system integration. Therefore, the thermal-hydraulic analysis presented herein is expected to provide valuable fundamental insights

contributing to a more holistic evaluation of marine nuclear reactor steam generator designs.

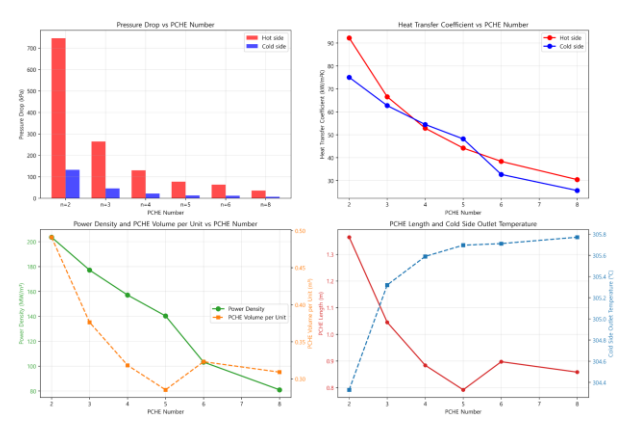


Fig. 4. Summary of the effects of the number of PCHE; pressure drop, HTC, power density and PCHE length

#### 3. Conclusions

This study performed a thermal-hydraulic sizing analysis for a PCHE-type steam generator in marine nuclear reactors, using validated two-phase flow correlations. Our findings reveal that the number of PCHE blocks significantly impacts performance, presenting a clear trade-off: fewer blocks enhance heat transfer efficiency and power density but increase pressure drop. Conversely, more blocks reduce pressure drop and overall length at the cost of lower efficiency. The analysis highlights the critical influence of mass flux on heat transfer and CHF. Ultimately, optimal marine reactor steam generator design requires integrating this thermal-hydraulic assessment with practical engineering considerations such as allowable pressure drop and maintenance requirements. In the context of marine nuclear propulsion, the compact design of a PCHE is a key advantage, as space constraints on a vessel are directly tied to economic viability and operational efficiency. The high-power density and heat transfer efficiency of PCHEs make them an excellent alternative to conventional steam generators, which often pose a significant volumetric challenge. Furthermore, the use of mini channels in PCHEs is expected to mitigate the effects of ship motion, as gravity's influence on fluid flow is significantly reduced at this scale. This inherent characteristic makes PCHEs particularly well-suited for the dynamic environment of a ship, offering a robust and stable solution for a nuclear-powered propulsion system.

# Acknowledgement

This work was supported by the National Research Foundation of Korea (NRF) grant funded by Korea government (MSIT) (RS-2025-02310831)

#### REFERENCES

[1] Kim, S. M., & Mudawar, I. (2013). Universal approach to predicting saturated flow boiling heat transfer in mini/micro-channels – Part II. Two-phase heat transfer coefficient.

International Journal of Heat and Mass Transfer, 64, 1239–1256.

- [2] Bertsch, S. S., Groll, E. A., & Garimella, S. v. (2009). A composite heat transfer correlation for saturated flow boiling in small channels. *International Journal of Heat and Mass Transfer*, 52(7–8), 2110–2118.
- [3] Shah, M. M. (1982). Chart correlation for saturated boiling heat transfer: Equations and further study. *ASHRAE Transactions*.
- [4] Gungor, K. E., & Winterton, R. H. S. (1986). A general correlation for flow boiling in tubes and annuli. *International Journal of Heat and Mass Transfer*, 29(3), 351–358.
- [5] Chen, J. C. (1966). Correlation for Boiling Heat Transfer to Saturated Fluids in Convective Flow. *Industrial & Engineering Chemistry Process Design and Development*, 5(3), 322–329.
- [6] Tran, T. N., Wambsganss, M. W., & France, D. M. (1996). Small circular- and rectangular-channel boiling with two refrigerants. *International Journal of Multiphase Flow*, 22(3), 485–498.
- [7] Jens, W. H., & Lottes, P. A. (1951). ANALYSIS OF HEAT TRANSFER, BURNOUT, PRESSURE DROP AND DENSITY DATE FOR HIGH- PRESSURE WATER.
- [8] Bang, K. H., Kim, K. K., Lee, S. K., & Lee, B. W. (2011). Pressure effect on flow boiling heat transfer of water in minichannels. *International Journal of Thermal Sciences*, 50(3), 280–286.
- [9] Groeneveld, D. C., Cheng, S. C., & Doan, T. (1986). 1986 AECL-UO critical heat flux lookup table. *Heat Transfer Engineering*, 7(1–2), 46–62.
- [10] Groeneveld, D. C., Shan, J. Q., Vasić, A. Z., Leung, L. K. H., Durmayaz, A., Yang, J., Cheng, S. C., & Tanase, A. (2007). The 2006 CHF look-up table. *Nuclear Engineering and Design*, 237(15-17 SPEC. ISS.), 1909–1922.
- [11] Yu, W., France, D. M., Wambsganss, M. W., & Hull, J. R. (2002). Two-phase pressure drop, boiling heat transfer, and critical heat flux to water in a small-diameter horizontal tube. *International Journal of Multiphase Flow*, 28(6), 927–941.
- [12] Lezzi, A. M., Niro, A., & Beretta, G. P. (1994). EXPERIMENTAL DATA ON CHF FOR FORCED CONVECTION WATER BOILING IN LONG HORIZONTAL CAPILLARY TUBES. *Proceeding of International Heat Transfer Conference* 10, 491–496.
- [13] Dougall, R. S., & Ronsenow, W. M. (1963). FILM BOILING ON THE INSIDE OF VERTICAL TUBES WITH UPWARD FLOW OF THE FLUID AT LOW QUALITIES.
- [14] Shah, M. M., & Siddiqui, M. A. (2000). A general correlation for heat transfer during dispersed-flow film boiling in tubes. *Heat Transfer Engineering*, 21(4), 18–32.
- [15] Groeneveld, D. C., & Delorme, G. G. J. (1976). PREDICTION OF THERMAL NON-EQUILIBRIUM IN THE POST-DRYOUT REGIME. *Nuclear Engineering and Design*, *36*, 17–26.
- [16] A.E. Dukler, M. Wicks, R.G. Cleaveland, Pressure drop and hold up in two-phase flow, AIChE J. 10 (1964) 38–51.
- [17] McAdams, W. H., Woods, W. K., & Heroman, L. C. (1942). Vaporization Inside Horizontal Tubes—II Benzene-Oil Mixtures. *Journal of Fluids Engineering*, *64*(3), 193–199.
- [18] A. Cicchitti, C. Lombardi, M. Silvestri, G. Soldaini, R. Zavalluilli, Two-phase cooling experiments-pressure drop, heat transfer and burnout measurements, Energia Nucleare 7 (1960) 407–425.
- [19] Mishima, K., & Hibiki, T. (1996). Some characteristics of air-water two-phase flow in small diameter vertical tubes. *International Journal of Multiphase Flow*, 22(4), 703–712.
- [20] L. Friedel, Improved friction pressure drop correlations for horizontal and vertical two-phase pipe flow, European Two-Phase Group Meeting, Ispra, Italy, 1979, Paper E2.

- [21] Sun, L., & Mishima, K. (2009). Evaluation analysis of prediction methods for two-phase flow pressure drop in minichannels. *International Journal of Multiphase Flow*, 35(1), 47–54.
- [22] Müller-Steinhagen, H., & Heck, K. (1986). A simple friction pressure drop correlation for two-phase flow in pipes. *Chemical Engineering and Processing: Process Intensification*, 20(6), 297–308.
- [23] Tanase, A., Cheng, S. C., Groeneveld, D. C., & Shan, J. Q. (2009). Diameter effect on critical heat flux. *Nuclear Engineering and Design*, 239(2), 289–294.